SiO_2 Nanowires Growing on Hexagonally Arranged Circular Patterns Surrounded by TiO_2 Films

Xiaohong An, Guowen Meng,* Qing Wei, Mingguang Kong, and Lide Zhang

Key Laboratory of Materials Physics, and Anhui Key Laboratory of Nanomaterials and Nanostructures, Institute of Solid State Physics, Chinese Academy of Sciences, Hefei 230031, P. R. China

Received: September 26, 2005; In Final Form: November 1, 2005

An effective approach has been demonstrated for the synthesis of novel composite architectures, SiO_2 nanowires (NWs) growing on hexagonally arranged circular patterns surrounded by TiO_2 films on Si substrate. First, a solution-dipping template strategy is used to create TiO_2 films with hexagonally arranged pores on Au-coated Si substrate, resulting in hexagonally arranged circular patterns of catalysts surrounded by TiO_2 films. Then the patterned catalysts guide the growth of SiO_2 NWs with the original TiO_2 films preserved, realizing the composite structures. Such composite architectures combine the photoluminescence (PL) properties of the two components, and also present more favorable PL property, laying a foundation for future advanced nano-optoelectronic devices.

Introduction

Current challenges in the synthesis of one-dimensional (1D) nanomaterials essentially comprise the controls over a single nanowire (NW) and the assembly of an ensemble of NWs. As far as a single NW is concerned, the control of morphology, size, and orientation is of paramount importance. For an ensemble of NWs, suitable arrangement on a substrate is critical to the realization of integrated electronic and photonic nanotechnology. Many methods have been developed for the fabrication of NW arrays, including a template-based method,[1−4] catalyst-guided growth,[5−10] Langmuir−Blodgett and fluidic alignment techniques,[11,12] and electrospinning.[13] Among them, catalyst-guided growth is the most effective method to synthesize orderly arranged nanotubes (NT)/NW architectures in desired patterns on a substrate, which have potential applications in flat panel displays, nanoelectronics, nanosensors, and skeletal templates for nanocomposites. Orderly arranged carbon NTs[5−9] and ZnO NWs[10] on different patterns have been fabricated by this method.

Silicon oxide (SiO_2), an important candidate material for photoluminescence (PL), has been studied for a long time. Because nanomaterials attract more and more attention due to their importance to the study of size- and dimensionality-dependent chemical and physical properties and great potential for nanoscale electronics and optoelectronics,[14,15] chemists and material scientists have fabricated various nanostructures of SiO_x, such as silica "nanoflowers",[16,17] radial patterns of carbonated silica fibers,[18,19] silica NW "bundles" and "nanobrush" arrays and silica nanotubes,[20] and treelike and tadpole-like SiO_x nanostructures.[21] Very recently, Liu et al.[22] have synthesized ultralong and highly oriented silicon oxide NWs by using Ga as catalysts; Pan and co-workers push the conventional VLS mechanism to a new range by using molten gallium as catalysts to grow highly aligned silica NWs.[23] However, there have been no reports on the fabrication of silica NW architectures on periodically arranged patterns on planar substrate.

Here, we demonstrate the catalyst-guided growth of SiO_2 NWs on hexagonally arranged circular patterns surrounded by TiO_2 films on Si substrate, realizing novel composite architectures. The method might be exploited to grow NWs of desired materials (such as semiconductor and insulator) on hexagonally arranged circular patterns, surrounded by films of other materials on a planar substrate by rationally selecting catalysts and the precursor solution of the films, and effectively controlling the conditions for the NW growth. The obtained composite architectures combine the properties of the two components and present new favorable properties. The films surrounding the NWs on hexagonally arranged circular patterns possess orderly arranged pores and may play important roles in many fields, such as photocatalysis,[24] gas sensors,[25] photonics,[26] optoelectronic devices,[27] and surface enhanced Raman scattering,[28] while the NWs on hexagonally arranged circular patterns have potential applications in sensor arrays and optoelectronic devices.[10]

Experimental Section

The novel composite architectures have been synthesized by a combination of solution-dipping template strategy[29] and subsequent catalyst-guided growth of NWs. Figure 1 is a schematic illustration of the process.

Monolayer Self-Assembled Arrays of Monodispersed Polystyrene Spheres (PSs). Centimeter square sized monolayer colloidal crystal was prepared on a clean glass substrate by spin-coating monodispersed polystyrene (PS) suspensions in a custom-built spin-coater.[30] For this, monodispersed PS suspensions were bought from Alfa Aesar Corporation. The concentration of the suspensions was 10% PS with diameters of 1 μm.

Hexagonally Arranged Circular Patterns of Au Catalysts Surrounded by TiO_2 Films on Planar Si Substrate. Au films were thermally evaporated onto a clean Si substrate. Then the monolayer colloidal crystal was transferred onto the Au side of the Si substrate by lifting off in water.[31] After being dried at room temperature, the Au-coated Si substrate with the monolayer colloidal crystal was heated at 120 °C for 6 min. After

* Corresponding author. E-mail: gwmeng@issp.ac.cn.

10.1021/jp055463b CCC: $33.50
Published on Web 12/06/2005

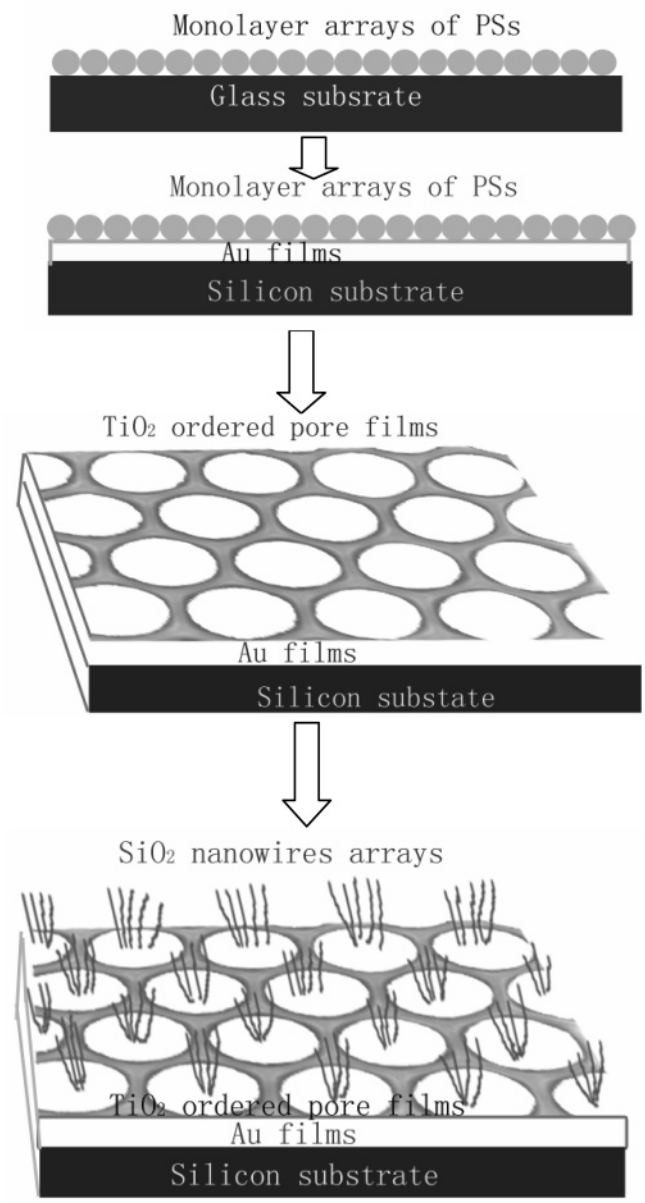

Figure 1. Schematic illustration for the formation of the composite architectures of SiO_2 NWs growing on the hexagonally arranged circular patterns surrounded by TiO_2 films on Au-coated Si substrate.

cooling to room temperature, a drop of presynthesized TiO_2 solution with a quantitative pipet was dipped into the void interstice of the monolayer colloidal crystal on the Au-coated Si substrate. For this, TiO_2 solution was prepared by hydrolyzing titanium tetraisopropoxide (15 mL) in ethanol (60 mL) at room temperature. Then the sample was put into an oven horizontally and dried at 80 °C for 30 min, followed by being solved in CH_2Cl_2 for 1 min to remove the PSs. Finally, rinsing and drying were performed for the solved samples before scanning electron microscopy (SEM) characterization.

Growth of SiO_2 NWs on Hexagonally Arranged Circular Patterns of Au Catalysts Surrounded by TiO_2 Films on Si Substrate. By using the patterned catalysts, SiO_2 NWs were grown by a catalyst-guided technique. Mg_3N_2 powers (99.9 wt %, 1 g) loaded in a ceramic boat were put into a horizontal ceramic tube (inner diameter 25 mm; length 80 cm) mounted inside a tube furnace. The obtained Au-coated Si substrate with planar porous TiO_2 films was placed at the downstream side of the source materials at a distance of about 2 cm. The furnace was heated from room temperature to 960 °C in 10 min and

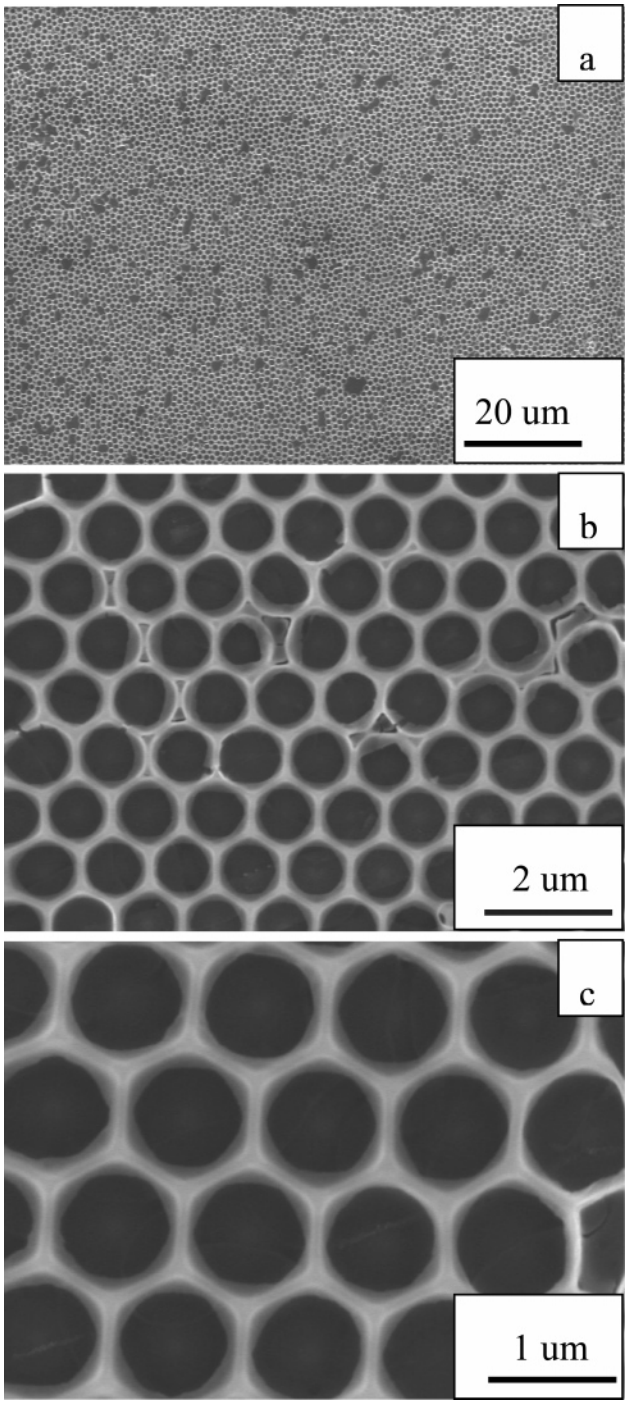

Figure 2. SEM images of the hexagonally ordered arrays of patterned catalysts surrounded by the TiO_2 films on Au-coated Si substrate.

maintained at this temperature for 70 min to grow SiO_2 NWs. High-purity Ar (99.99 wt %, $O_2 \sim 0.01$ wt %) with a flow rate of 5 mL/min was introduced into the ceramic tube during the experiment. The temperature of the Au-coated Si substrate is about 930 °C, determined by a premeasured temperature gradient curve. After the furnace was cooled to room temperature, white products were found on the Au-coated Si substrate with TiO_2 films. The final white products were characterized by SEM (Sirion 200), transmission electron microscopy (TEM, Hitachi 800 at 200kv), energy-dispersive X-ray spectroscopy (EDX) attached to the TEM, and X-ray diffraction (XRD, X'Pert Pro MPD). Photoluminescence spectra were recorded on a LabRam-HR micro-Raman spectrometer (Jobin-Yvon).

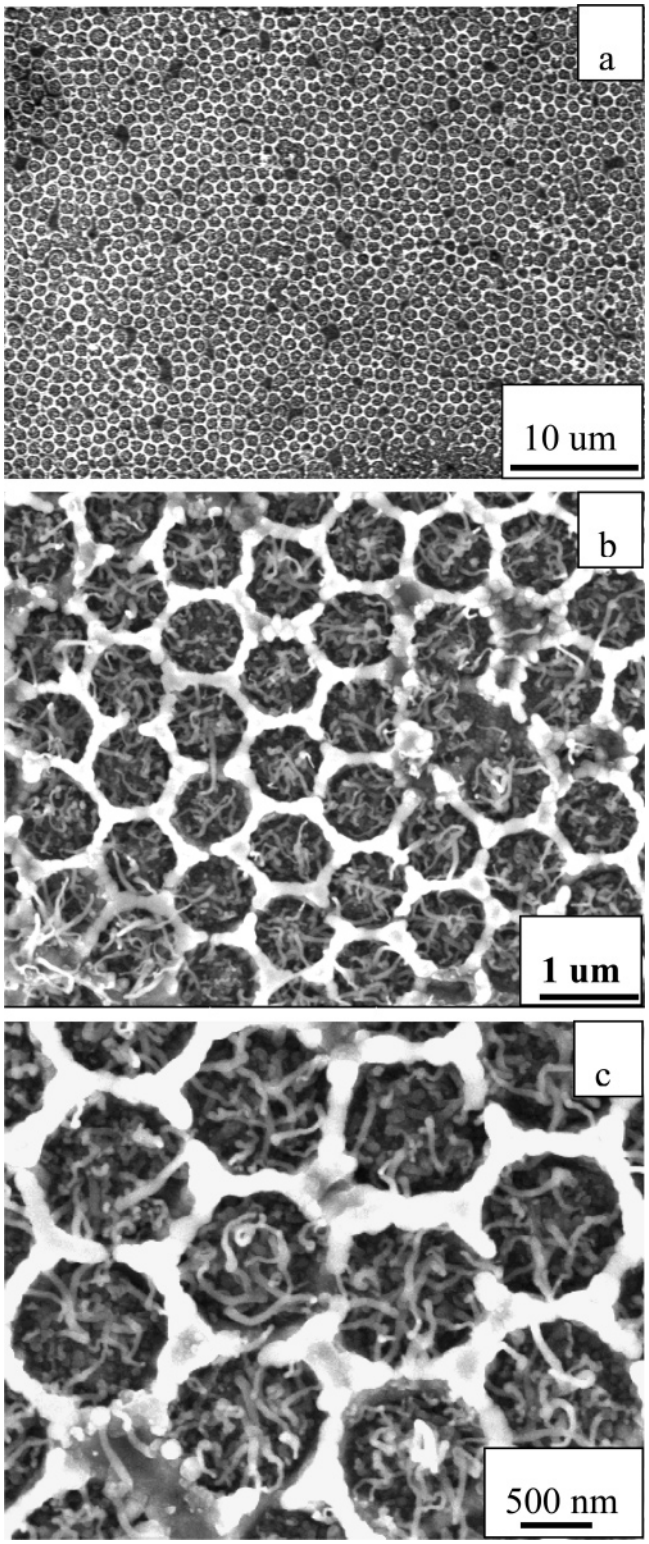

Figure 3. SEM images of the composite structures of SiO_2 NWs on the hexagonally arranged circular patterns surrounded by TiO_2 films

Results and Discussion

Different magnification SEM images of the TiO_2 films with hexagonally arranged pores on the Au-coated Si substrate are shown in Figure 2. XRD analysis has confirmed that the films consist of crystalline anatase TiO_2 (not shown here). Figure 2a shows that a large area of TiO_2 porous films with a thickness about 100 nm is obtained. From Figure 2b−c, it can be seen that the pores in the TiO_2 films were hexagonally arranged on the Au-coated Si substrate, and the center-to-center distance between the adjacent pores is about 1 μm, consistent with the diameter of the PSs used. Because the planar TiO_2 porous films were formed on the Au-coated Si substrate, the Au films underneath (fully covered by) the TiO_2 films will have no effect on the growth of NWs. However, the Au films inside the pores in the TiO_2 films are exposed and will guide the growth of SiO_2 NWs.

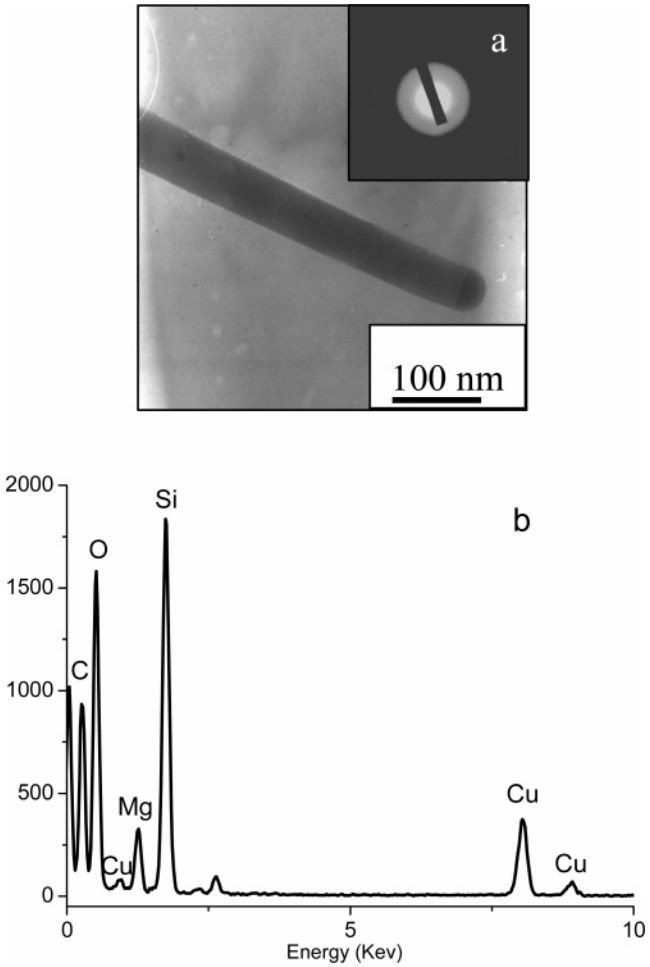

Figure 4. (a) Low-magnification TEM image of a typical SiO_2 NW; (b) EDX spectra taken from the SiO_2 NW.

An SEM top view of the final composite architectures (Figure 3a) reveals that the honeycomblike arrangement of the TiO_2 films was preserved after the growth of NWs. A magnified SEM observation (Figure 3b) demonstrates that the NWs were grown only on the hexagonally arranged pore areas, with no NWs growing on the TiO_2 films surrounding the pores. A close-up view (Figure 3c) shows that the NWs are about 500 nm high and 50 nm in diameter. There are round nanoparticles on the ends of most NWs, indicating that the NWs were formed through a vapor−liquid−solid (VLS) growth model.

TEM observation (Figure 4a) of a typical NW also reveals that there exists a round particle at the tip (the round particle is darker than the NW stem). A selected area electron diffraction (SAED) pattern (inset of Figure 4a), recorded from the NW, shows diffuse rings, indicating that the NW is amorphous. The component of the NW was further confirmed by EDS analysis (Figure 4b), revealing that the NW is mainly composed of Si and O with an atomic ratio close to 1:2, with a little trace of Mg. The copper and carbon signatures are from the TEM copper grid with carbon films. Taken together, the NWs are mainly composed of SiO_2.

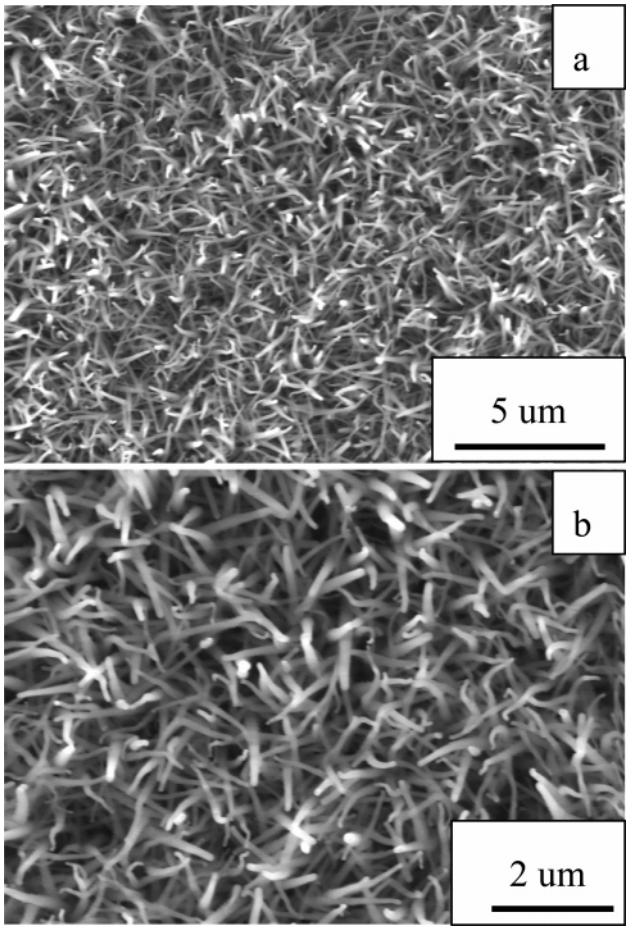

Figure 5. SEM images of the SiO_2 NWs arrays on Au-coated Si substrate without TiO_2 films.

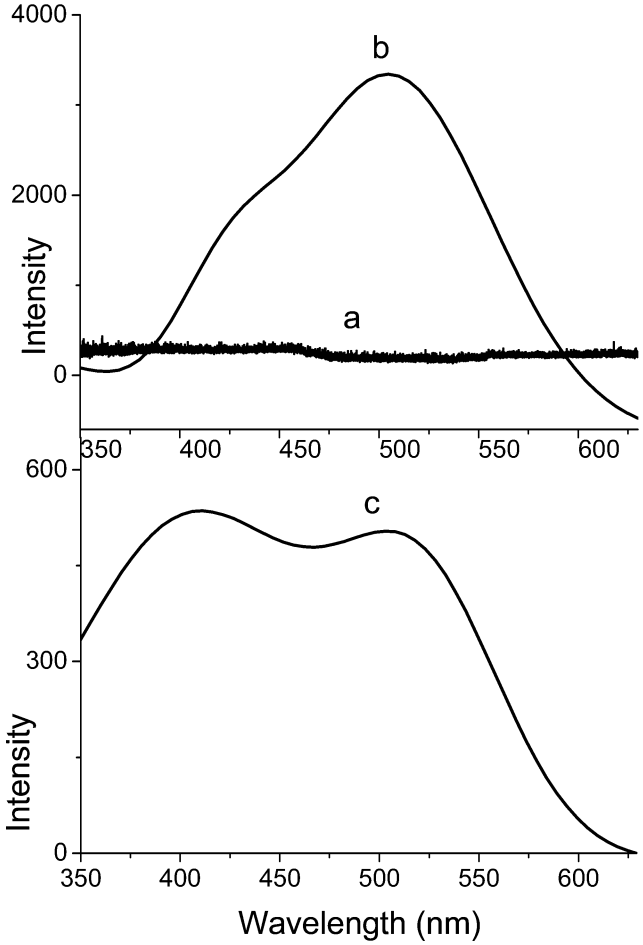

Figure 6. Photoluminescence spectrum from the planar bare TiO_2 porous films (a), the novel composite architectures (b), and the SiO_2 NWs arrays on Au-coated Si substrate without TiO_2 films (c).

The formation of the SiO_2 NWs is similar to that of highly aligned SiO_2 and silicon NWs.[23,32−36] When the Si substrate is heated to a high temperature, the Au film on the Si substrate inside the pores in the TiO_2 films breaks up to form Au nanoparticles. These Au nanoparticles etch the Si substrate to generate liquid Au−Si alloy nanodroplets. The Si atoms in the Au−Si alloy droplets evaporate to form a dense vapor of Si species around the Si substrate. At this stage, the vapor consists of Mg, O, Si, and N (Mg_3N_2 powers are oxidized, forming MgO, NO, and NO_2). The oxygen may come from (i) the oxide layer on the Si wafer, (ii) the residual oxygen in the reaction chamber, (iii) the Ar carrier gas, or (iv) the leakage of the vacuum system. Thus, the liquid Au nanodroplets can absorb Si and O species from the vapor. With the supply of more mixed-gas species, Si and O atoms in the Au nanodroplets become supersaturated and then separate out as SiO_2 on the surface of the Si substrate, acting as nucleation sites and initiate the growth of the SiO_2 NWs. The liquid droplets are then lifted up from the Si substrate by the growing NWs. During the SiO_2 NW growth, the liquid nanodroplets also absorb a little trace of Mg species from the mixed gas species. When the Au nanodroplets become supersaturated, Mg species separate out, together with Si and O, forming SiO_2 NWs doped with a little trace of Mg. The SiO_2 NWs could not grow on the TiO_2 films surrounding the pores because the TiO_2 films surrounding the pores covered the Au films, preventing the mixed gas species from contacting with Au films underneath the TiO_2 films. On the other hand, the planar TiO_2 films were preserved after the growth of NWs. Consequently, the composite structures of SiO_2 NWs growing on the hexagonally arranged circular patterns surrounded by TiO_2 films were obtained.

The composite architectures are composed of SiO_2 NWs on hexagonally arranged circular patterns surrounded by TiO_2 films, so their PL property may be affected by the two components. For this study, we compare the PL property of the composite architectures with that of the hexagonally arranged porous planar TiO_2 films on the Si substrate (after being heated at 960 °C) and also with that of the SiO_2 NW arrays on Au-coated Si substrate without TiO_2 films, which were grown under the same conditions as those for SiO_2 NWs on Au-coated Si substrate with porous TiO_2 films. Figures 5a and b are the SEM images of the SiO_2 NW arrays. It can be seen that all the NWs densely stand on the Au-coated Si substrate and form self-oriented NW arrays.

PL spectra (Figure 6) from the planar bare TiO_2 porous films, the composite architectures, and the SiO_2 NW arrays have been recorded with the excitation wavelength of 325 nm. There is no emission peak for the bare TiO_2 porous films (curve 6a), indicating that the bare TiO_2 porous films have no PL emission. As for the composite architectures (curve 6b) and the SiO_2 NW arrays (curve 6c), there are two similar peaks, a blue one centered at 414 nm and a green one at 509 nm, indicating that the composite architectures preserve the PL property of the SiO_2 NWs. The green emission band (509 nm) could be attributed to the radiative recombination from the defect centers in the silica, such as oxygen vacancies.[37] The emission peak at 414 nm possibly corresponds to some intrinsic diamagnetic defect centers in the SiO_2 NWs, such as 2-fold coordinated silicon

lone-pair centers (O−Si−O).[38] Compared with those of the SiO_2 NW arrays (curve 6c), the intensity of the 509 nm emission increases and the relative intensity of 414 nm emission decreases for the composite architectures (curve 6b). Because no other emission is evident at lower energy, it can be concluded that the composite architectures, SiO_2 NWs on hexagonally arranged circular patterns surrounded by TiO_2 films, either alter or destroy the defect configurations responsible for the 414 nm emission or they create diamagnetic defects that offer competing radiative recombination channels. On the other hand, the obvious increase (about 7 times) of the absolute PL emission for the composite architectures (curve 6b) reveals that the TiO_2 films may be useful for the increase of the absolute PL emission. But how the TiO_2 films affect the absolute PL emission is still under study. Taken together, the composite architectures can not only combine the PL properties of the two components, but also present more favorable PL property, which may have potential applications in future nano-optoelectronic devices.

Conclusion

In summary, the composite structures, SiO_2 NWs growing on hexagonally arranged circular patterns surrounded by TiO_2 films on Au-coated Si substrate, have been obtained by a solution-dipping template strategy followed by catalyst-guided growth of NWs. The synthetic route presented here is universal and can be exploited to synthesize NWs of desired materials on hexagonally arranged circular patterns surrounded by films of other materials on planar substrate by rationally selecting catalysts and the precursor solution of the films and effectively controlling the conditions for the NW growth. We have synthesized a variety of hexagonally arranged pore films of other materials, such as, ZnO, Fe_2O_3, SiO_2, etc., on planar substrates of other materials coated with different catalysts, on the basis of which patterned NWs of different materials can be grown. The SiO_2 NWs growing on the hexagonally arranged circular patterns surrounded by TiO_2 films on Au-coated Si substrate can not only combine the PL properties of the two components, but also present more favorable PL emission, laying a foundation for realizing advanced nano-optoelectronic devices. On the other hand, the preservation of the ordered porous TiO_2 films makes the composite structures possible for applications in photocatalysis and gas sensors.

Acknowledgment. We are grateful for the financial support of Natural Science Foundation of China (Grants 10374092 and 50525207) and the Ministry of Sciences and Technology of China (Grant G1999064501)

References and Notes

(1) Brumlik, C. J.; Martin, C. R. *J. Am. Chem. Soc.* **1991**, *113*, 3174.
(2) Fan, R.; Wu, Y. Y.; Li, D. Y.; Yue, M.; Majumdar, A.; Yang, P. D. *J. Am. Chem. Soc.* **2003**, *125*, 5254.
(3) Limmer, S. J.; Cao, G. Z. *Adv. Mater.* **2003**, *15*, 427.
(4) Melosh, N. A.; Boukai, A.; Diana, F.; Gerardot, B.; Badolato, A.; Petroff, P. M.; Heath, J. R. *Science* **2003**, *300*, 112.
(5) Kempa, K.; Kimball, B.; Rybczynski, J.; Huang, Z. P.; Wu, P. F.; Steeves, D.; Sennett, M.; Giersig, M.; Rao, D. V. G. L. N.; Carnahan, D. L.; Wang, D. Z.; Lao, J. Y.; Li, W. Z.; Ren, Z. F. *Nano Lett.* **2003**, *3*, 13.
(6) Huang, Z. P.; Carnahan, D. L.; Rybczynski, J.; Giersig, M.; Senett, M.; Wang, D. Z.; Wen, J. G.; Kempa, K.; Ren, Z. F. *Appl. Phys. Lett.* **2003**, *82*, 460.
(7) Cao, A. Y.; Wei, B. Q.; Jung, Y.; Vajtai, R.; Ajayan, P. M.; Ramanath, G. *Appl. Phys. Lett.* **2002**, *81*, 1297
(8) Zhang, Z. J.; Wei, B. Q.; Ramanath, G.; Ajayan, P. M. *Appl. Phys. Lett.* **2000,** 77, 3764.
(9) Wei, B. Q.; Vajtai, R.; Jung, Y.; Ward, J.; Zhang, Y.; Ramanath, G.; Ajayan, P. M. *Nature* **2002**, *416*, 495.
(10) Wang, X. D.; Summers, C. J.; Wang, Z. L. *Nano Lett.* **2004**, *4*, 423.
(11) Huang, Y.; Duan, X. F.; Wei, Q. Q.; Lieber, C. M. *Science* **2001**, *291*, 630.
(12) Yang, P. D. *Nature* **2003**, *425*, 243.
(13) Li, D.; Wang, Y. L.; Xia, Y. N. *Nano Lett.* **2003**, *3*, 1167.
(14) Han, J.; Fan, S.; Li, Q.; Hu, Y. *Science* **1997**, *277*, 1287.
(15) Ruecks, T.; Kim, K.; Joselevich, E.; Tseng, G. Y.; Cheung, C.; Lieber, C. M. *Science* **2000**, *289*, 94
(16) Zhu, Y. Q.; Hsu, W. H.; Terrones, M.; Grobert, N.; Terrones, M.; Hare, J. P.; Kroto, H. W.; Walton, D. R. M. *J. Mater. Chem.* **1998**, *8*, 1859.
(17) Zhu, Y. Q.; Hu, W. B.; Hsu, W. H.; Terrones, M.; Grobert, N.; Karali, T.; Terrones, M.; Hare, J. P.; Townsend, P. D.; Kroto, H. W.; Walton, D. R. M. *Adv. Mater.* **1999**, *11*, 844.
(18) Zhang, Z. J.; Ramanath, G.; Ajiayan, P. M.; Goldberg, D.; Bande, Y. *Adv. Mater.* **2001**, *13*, 197.
(19) Zhang, Z. J.; Ajiayan, P. M.; Ramanath, G. *Appl. Phys. Lett.* **2001**, *78*, 3794.
(20) Wang, Z. L.; Gao, R. P.; Gole, J. L.; Stout, J. D. *Adv. Mater.* **2000**, *12*, 1938.
(21) Chen, Y. J.; Li, J. B.; Dai, J. H. *Chem. Phys. Lett.* **2001**, *344*, 450.
(22) Zheng, B.; Wu, Y. Y.; Yang, P. D.; Liu, J. *Adv. Mater.* **2002**, *14*, 122.
(23) Pan, Z. W.; Dai, Z. R.; Ma, C.; Wang, Z. L. *J. Am. Chem. Soc.* **2002**, *124*, 1817.
(24) Matsushita, S. I.; Miwa, T.; Tryk, D. A.; Fujishima, A. *Langmuir* **1998,** *14*, 6441.
(25) Elizabeth, C. D.; Oomman, K. V.; Keat, G. O. *Sensors* **2002**, *2*, 91.
(26) Yablonovitch, E.; Gmitter, T. J.; Meade, R. D.; Rappe, A. M. *Phys. Rev. Lett.* **1991,** *67*, 80.
(27) Imada, M.; Noda, S., Chutinan, A.; Tokuda, T. *Appl. Phys. Lett.* **1999**, *75*, 316.
(28) Tessier, P. M.; Velev, O. D.; Kalambur, A. T. *Adv. Mater.* **2001**, *13*, 396.
(29) Sun, F. Q.; Cai, W. P.; Li, Y.; Cao, B. Q.; Lei, Y.; Zhang, L. D. *Adv. Funct. Mater.* **2004**, *14*, 283.
(30) Haynes, C. L.; McFarland, A. D.; Smith, M. T. *J. Phys. Chem. B* **2002**, *106*, 1898.
(31) Burmeister, F.; Schafle, C.; Leiderer, P. *Langmuir* **1997**, *13*, 2983.
(32) Dai, L.; You, L. P.; Duan, X. F.; Lian, W. C.; Qin, G. G. *Phys. Lett. A* **2005**, *335*, 304.
(33) Kar, S.; Chaudhuri, S. *Solid. State. Commun.* **2005,** *133*, 151.
(34) Pan, Z. W.; Dai, S.; Beach, D. B.; Lowndes, D. H. *Nano. Lett.* **2003,** *3*, 1279.
(35) Ma, R. Z.; Bando, Y. *Chem. Phys. Lett.* **2003**, *377*, 177.
(36) Yao, Y.; Li, F. H.; Lee, S. T. *Chem. Phys. Lett.* **2005**, *406*, 381.
(37) Liao, L. S.; Bao, X. M.; Zheng, X. Q.; Li, N. S.; Min, N. B. *Appl. Phys. Lett.* **1996**, *68*, 850.
(38) Yu, D. P.; Hang, Q. L.; Ding, Y.; Zhang, H. Z.; Bai, Z. G.; Wang, J. J.; Zou, Y. H.; Qian, W.; Xiong, G. C.; Feng, S. Q. *Appl. Phys. Lett.* **1998**, *73*, 3076.